

Kinesthetic feedback improves grasp performance in cable-driven prostheses

Michael E. Abbott*, Joshua D. Fajardo, H.W. Lim, and Hannah S. Stuart

Abstract—Despite significant progress in the realm of upper-limb prosthetic design, end-users still abandon modern myoelectric prostheses, with haptic feedback listed as a primary need. The passive scheme of cable-driven body-powered prostheses provides kinesthetic sensory information to the user but can also lead to discomfort and fatigue due to the large loads applied to the body during operation. In order to investigate the role of this kinesthetic feedback on grasp force control, we design a body-powered prosthesis emulator capable of varying the amount of displayed force feedback along a continuous scale. Using this experimental test bed, we collect data from 9 participants while they perform a grasp and lift task. Analysis shows that, with increasing amounts of force feedback, people produce lower and steadier grasp forces but also become more prone to dropping held objects. These results suggest that the use of moderate amounts of feedback provides significant grasp performance benefits while also mitigating some of the shortcomings of cable-driven prostheses. These findings support the continued study of the incorporation of kinesthetic feedback into novel prosthetic designs.

I. INTRODUCTION

The absence of a hand negatively impacts a person’s ability to perform activities of daily living (ADLs) [1], [2]. Replicating the dexterous capabilities of the human hand, with its numerous afferent and efferent neural pathways, continues to be a challenge for prosthetists and robotics researchers alike. For functional prostheses (i.e. not purely cosmetic), individuals generally choose between two classes of devices with distinct modes of operation: myoelectric and body-powered. Myoelectric arms are active devices which typically use DC motors for actuation and detect user intent through the use of surface electromyography (sEMG) electrodes placed on the skin. Body-powered devices instead passively couple the end effector to the contralateral shoulder through a shoulder harness and Bowden cable system.

Significant recent research seeks to improve and modernize prosthetic technologies. Many of these efforts focus on adding dexterity via degrees of actuation to actively driven hands, like the bebionic [3] and i-Limb Ultra [4] hands, or reducing cost of electromechanical devices, as with the Hero Arm [5]. Rejection rates for these types of motorized devices have been estimated at between 33% and 50% [6]. Surveys of myoelectric prosthesis users and rejecters consistently rate the addition of feedback modalities and more predictable control as top priorities in the technology [7]. Prior research

explores the addition of haptic displays in prostheses, such as compact sensory substitution methods using vibrotactile or electrotactile stimulation, e.g., [8]–[11], while other systems aim to match sensed and feedback modalities, e.g. locally applied body loads in [12], [13]. These technologies are typically presented as add-ons to myoelectric prostheses and are distinct from the device control scheme. This can hinder interaction transparency and efficiency and may contribute to why these technologies are not yet adopted widely.

Despite possessing a design largely unchanged over the past 75 years, body-powered cable-driven grippers allow for more robust control and feedback through passive actuation [14], [15]. The mechanical connection between a user’s shoulder and the end effector provides kinesthetic feedback to the user in the forms of both position and force. This enables the development of internal models which map motor inputs at the shoulder to actions of the end effector, for improved grasping performance [16]. The co-location of the control and feedback modalities also aids in the integration of the sensory information for the user [17]. This control topology was formalized as extended physiological proprioception (EPP) by D.C. Simpson [18] and shown to exhibit superior feedforward and feedback information rates over alternative control mappings [19].

However, body-powered prostheses can produce discomfort and fatigue that accompany the body forces inherent to this passive system [6], [7]. We aim to understand the relationship between kinesthetic feedback and user exertion as well as the associated trade-offs for advanced prosthesis design. This work expands upon the findings of previous works which have investigated the benefits of kinesthetic feedback on grasping with upper-limb prosthetic devices [20], [21] with several distinctions. While prior efforts present feedback conditions in a binary fashion (i.e. feedback on or off), we vary force feedback along a continuous scale to gain insight into trends in grasp performance over a range of force feedback levels. Additionally, we evaluate grasp performance primarily through applied grasp forces during a grasp and lift task, as opposed to decision-oriented tasks such as haptic discrimination. To the authors’ knowledge, this work represents the first effort to quantify the effect of a continuously varying range of force feedback levels on grasp force control in upper-limb body-powered prostheses.

A. Overview

We present experimental results from a series of grasp and lift trials with participants operating a new haptic test bed designed to emulate a body-powered prosthesis. In

M.E. Abbott, J.D. Fajardo, and H.S. Stuart are with the Embodied Dexterity Group, Dept. of Mechanical Engineering, University of California Berkeley, Berkeley, CA, USA.

H.W. Lim is with the Dept. of Mechanical Engineering, University College London, London, England.

* Corresponding author (email: michael_abbott@berkeley.edu)

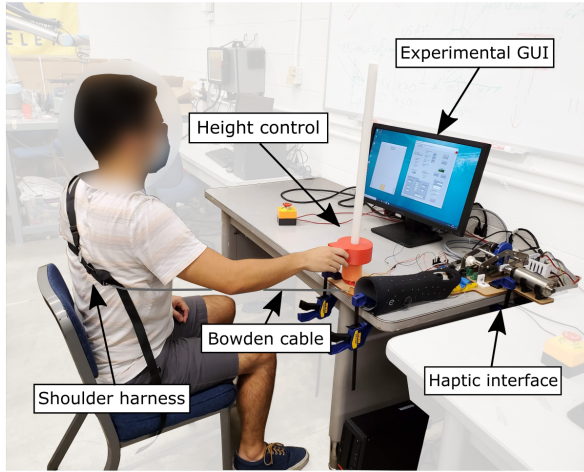


Fig. 1. A haptic interface mediates interactions between a participant and a virtual grasping environment, where the individual completes an experimental grasp-lift task using the shoulder harness and height controller. The haptic interface displays varying amounts of force feedback relative to the grasp state of the environment to evaluate its role in grasp force control.

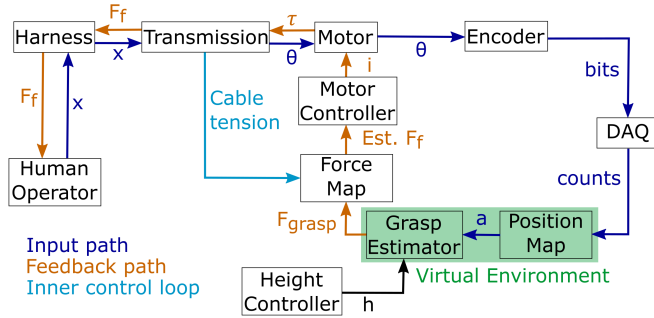


Fig. 2. Block diagram for operation of the experimental test bed. Participants impart some cable excursion x that is converted to a change in angle of the motor shaft θ through the haptic interface. The virtual environment maps this angle to a gripper aperture a which is used to calculate a grasp force F_{grasp} . A force map outputs a target feedback force F_f that is displayed to the user as a force pulling on the shoulder harness through energizing the motor coils with a current i . An inner control loop uses a tension sensor at the output of the transmission to reduce any error between intended and actual applied forces.

Section II, we introduce the elements and parameters of our experimental test bed. Section III discusses the protocol used during the human subject experiment, as well as the performance metrics and statistical methods used for analysis. Results presented in Section IV show that force feedback results in steadier and more efficient grasps, with potential implications on integration into wearable technologies discussed in Section V. We conclude in Section VI with future directions for the study of kinesthetic feedback and its potential applications.

II. TEST BED DESIGN

In order to systematically vary the magnitude of force feedback provided to participants during a grasping experiment, we developed a test bed, pictured in Fig. 1 and outlined in Fig. 2, comprised of three main components: a shoulder

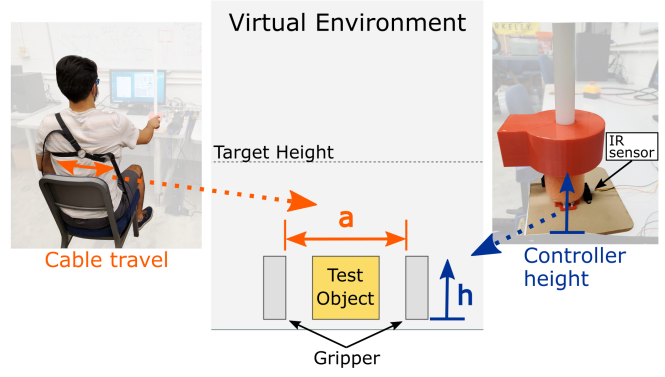


Fig. 3. Inputs to and operation of the virtual grasping environment. Travel of the cable, actuated through adduction and abduction of the shoulder blades, controls the aperture of the virtual gripper and resulting grasp force. Movement of the height controller, as measured by an IR distance sensor, changes the height of the virtual gripper.

harness actuated by a haptic interface, an experimental graphical user interface (GUI), and an object height controller.

A. Participant Control Inputs

Participants physically interact with two system components to complete the experimental grasping task. The first is a figure-of-nine upper-limb body-powered prosthesis harness worn around the left shoulder of the participant, pictured in Fig. 1 and the left of Fig. 3. A Bowden cable, with one end terminating on the harness and the other attached to the haptic interface, transmits positions and forces to and from the user during operation of the device. A cable routing element mounted to the tabletop limits extraneous motion of the Bowden cable.

The height controller, pictured in Fig. 1 and on the right of Fig. 3, provides an additional control input to the virtual grasping environment. Participants raise and lower a 3D-printed element along a PTFE guide tube, whose height is measured with an IR range sensor (Sharp GP2Y0A21YK0F) mounted to the base.

B. Virtual Environment

The experimental GUI presents the participant with a visualization of the virtual grasping environment containing a test object (yellow) and two opposed sides of a gripper (grey), both pictured in Fig. 3. The virtual environment provides an experimental focus on the primary variable of interest, force feedback through the Bowden cable, and avoids potential confounds present in physical interactions such as weight-based grasp adjustments. Excursion of the cable, as measured by the rotary encoder fixed to the motor shaft, opens the aperture, a , of the gripper. The level of the height controller controls the height of the gripper h .

We simulate the object-gripper interactions and object dynamics to inform both the GUI display and harness force control. The calculation of grasp force, F_{grasp} , is:

$$F_{grasp,i} = \begin{cases} 0 & a_i \geq w \\ k_c \frac{(w-a_i)}{2} & a_i < w \end{cases} \quad (1)$$

where k_c is the contact stiffness, a_i is the current aperture of the gripper, and w is the width of the test object. The simulation only applies this equation when the gripper height is aligned with the height of the object. Motion of the test object is limited to the vertical direction and defined by the following dynamic model:

$$\ddot{y}_{block,i} = \begin{cases} \ddot{y}_{gripper,i} & \text{no slip} \\ \frac{1}{m} (2\mu F_{grasp,i}) - g & \text{slip} \end{cases} \quad (2)$$

where g is the acceleration due to gravity, m is the object mass, and slip is defined as occurring when the grasp force is not high enough to produce sufficient friction force, with a maximum magnitude of $\mu F_{grasp,i}$, to resist the inertial and gravity loads on the test object.

We select environment parameters to simulate a typical grasping task. We define the block to have a mass m of 1 kg, width w of 4 cm, and a coefficient of friction μ of 0.7. We also define the contact stiffness between the block and gripper to be 10 kN/m. This configuration results in a minimum grasp force of 7 N for object lift-off and is used for all experiments.

C. Haptic Interface

A close-up view of the haptic interface assembly is shown in Fig. 4. A brushless DC (BLDC) motor (Maxon, EC-i 52) provides the torque necessary to transmit feedback forces to the participant. An incremental rotary encoder (Maxon, ENC Easy 16) measures rotation of the motor shaft, related to linear travel of the carriage through the cable transmission. A Maxon EPOS4 Compact 50/8 digital positioning controller handles all motor control aspects, including current control of the motor and reading of encoder values. The force feedback that is output by the motor for a given time step i is governed by a differential PI controller, such that:

$$u_i = u_{i-1} + \Delta u_{FF,i} + K \left(\Delta e_i + \frac{\Delta t_i}{\tau} e_i \right) \quad (3)$$

where u is the commanded current to the motor, u_{FF} is the feedforward current predicted by the transmission model, K is the controller gain, τ is the integral time constant, and Δt is the time step. The error e is the difference between the force target, i.e. the virtual grasp force F_{grasp} adjusted by the force feedback factor K_f , and the measured tension force in the Bowden cable:

$$e_i = K_f F_{grasp,i} - F_{sensor,i} \quad (4)$$

Varying K_f provides the ability to change the level of force feedback presented to the user and is the primary independent variable of study in this work.

A two-stage cable transmission uses a system of capstans, pulleys and a linear stage. The first reduction stage (colored in purple and blue in Fig. 4) amplifies the torque output of the system by a factor of 1.98. Two tensioned cables wrapped around both pulleys in a figure-eight pattern allow bidirectional transmission of torque. The second stage (colored in yellow and green) translates between the rotary motion of

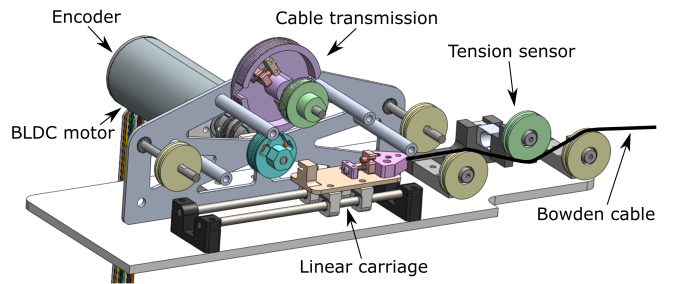


Fig. 4. Cross-sectional view of the haptic interface assembly with key elements labeled. The Bowden cable from the harness terminates on a linear carriage which constrains its motion to a single degree of freedom. A cable transmission converts between the linear motion and force of the carriage and rotary motion and torque of the attached brushless DC (BLDC) motor. An encoder fixed to the motor shaft measures rotation of the shaft. A custom tension sensor measures the forces applied to the participant through the Bowden cable from the torque output of the motor.

TABLE I
COMPARISON OF SYSTEM SPECIFICATIONS

	Prosthesis Standard [22]	Haptic Interface
Force (N)	62	70
Travel (mm)	50	97

the motor and the linear travel of the harness cable, which is attached to the linear carriage. All pulleys and brackets are made from 3D printed PLA and the mounting plates from laser cut carbon steel. A 5 kg load cell (HT Sensors, TAL220B) and a set of 3 offset pulleys measure the tension in the Bowden cable connecting the interface and shoulder harness. The deflection in the path of the cable caused by the offset pulleys results in a vertical force when the cable is under tension.

Evaluation of the test bed shows performance beyond the required force and travel for upper-limb body-powered prosthesis operation, summarized in Table I [22].

III. EXPERIMENTAL METHODS

A. Study Procedure

Participants sit in a chair facing a desk where the experimental apparatus is mounted. They don the shoulder harness which the experimenter then adjusted for proper fit. The haptic interface is initialized with the cable position fixed, and the participant is instructed to move the chair such that the cable is in tension with their shoulder blades in an adducted state. The participant is then given the opportunity to practice at the lowest ($K_f = 0$) and highest ($K_f = 1.33$) force feedback factors that will be displayed during the experiment in order to confirm comfort within the range of motion and force used in the study.

Each trial consists of a grasp and lift task modeled after similar grasp force studies performed with normative grasping [23]–[25]. The participant is instructed to grasp and lift the virtual object on the experimental GUI using the shoulder harness and height controller up to a height of at least 15 cm, noted by a dashed line. They must hold the object at or above this minimum height for a period

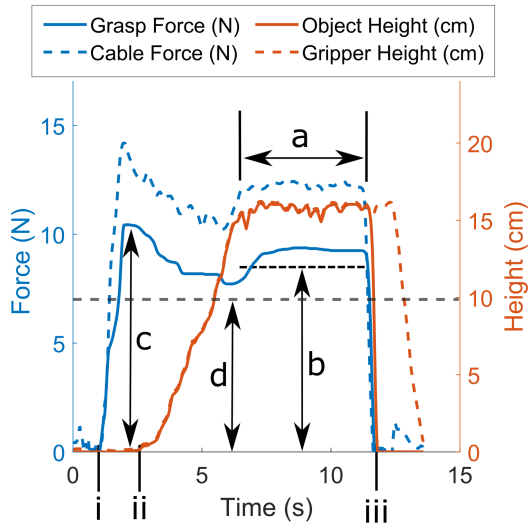


Fig. 5. Sample force and height data measured over time from a single grasping trial with a force feedback factor $K_f = 1.33$. Roman numerals mark key events during the trial: i) first virtual gripper contact with test object, ii) initiation of lift of the test object, and iii) release and descent of the test object. Letters denote key trial metrics and parameters: a) hold region, b) mean grasp force (averaged over the hold region), c) peak grasp force, and d) minimum grasp force to prevent slip.

of five seconds. The trial is completed when the subject releases the object and returns the virtual gripper back to the ground level. Visual indicators in the GUI provide guidance through each phase of the trial. Participants are instructed that the experiment evaluates only grasp force, not speed. Each participant completes grasping trials at five different force feedback factors: 0 (no feedback), 0.33 (light feedback), 0.67 (moderate feedback), 1 (equal feedback), and 1.33 (augmented feedback). Feedback factors, limited to 5 per participant due to time constraints, were selected to evenly span values between 0 and 1 along with one additional factor greater than 1 to examine the potential continuation of any observed trends. Ten trials are completed together at each feedback level, whose order is pseudorandomized through a Fisher-Yates shuffle. Participants are not notified of the feedback factor during any set of trials.

Data represent a total of 9 non-amputee participants with normative upper limb function. Participants were recruited from the student body of the UC Berkeley College of Engineering. All experimental procedures are approved by the University of California, Berkeley Institutional Review Board protocol #2019-05-12178.

B. Performance Metrics

Force and height data are recorded throughout each trial at a rate of 50 Hz – a single example trial is shown in Fig. 5. For each vector of force or height data x , we compute a local linear regression across a subset of 7 adjacent points beginning at each data point in the vector (i.e. $[x_i, x_{i+1}, \dots, x_{i+6}]$). Each set of data is then divided into phases with the following transition criteria:

- *Rise*: Slope is positive with absolute value greater than 5% of peak signal value

- *Plateau*: Slope has absolute value less than 1% of peak signal value
- *Fall*: Slope is negative with absolute value greater than 5% of peak signal value

Hold region is defined as the interval between the time of the first plateau and the final fall in object height signal while above the target height. If a plateau is not reached, the ascending and descending crossing times of the target height are used instead. We then calculate a range of metrics to characterize performance:

- *Mean grasp force*: mean grasp force for the hold region
- *Mean absolute deviation (MAD) of grasp force*: mean absolute deviation from the mean grasp force across the hold region
- *Peak grasp force*: maximum grasp force measured at any point during the trial
- *Drop trial*: trial with a hold region shorter than 95% of the hold time of 5 seconds¹
- *Number of probes*: number of rise changes in grasp force before the hold region
- *Number of lift attempts*: number of rise changes in object height before the hold region

C. Statistical Analysis

Due to observed within-subject correlation and the continuous nature of the data, linear mixed models (LMM) are used to separately relate the mean grasp force, peak grasp force, and mean absolute deviation in grasp force to the predictor variables. Force feedback factor (K_f) is added as a fixed effect as the primary predictor variable. The order in the sequence of feedback factors (factor order FO , ranging from 1 to 5) and in the sequence of trials (trial T , ranging from 1 to 10) are added as covariates, with trial nested within factor order. A first-order autoregressive ($AR(1)$) correlation structure is imposed to account for observed autocorrelation of lag 1. Participants are added as a random (slope and intercept) effect for all mixed models. Outcome variables are log-transformed prior to model fitting to normalize residuals.

Generalized linear models (GLM) capture the remaining non-continuous outcomes. A binomial logistic regression models drop chance and a Poisson regression is used to model the number of probes and lift attempts. Predictor variables are force feedback factor, factor order, and trial with the same nesting structure as above. No significant within-subject correlation is observed for the non-continuous outcomes, so no random effects for participants are included for model parsimony.

Model selection is performed using the Akaike Information Criterion (AIC) for all presented models. All analyses utilize R v3.6.2 [26] primarily with the "nlme" [27] and "lme4" [28] packages for linear mixed models and generalized linear models, respectively.

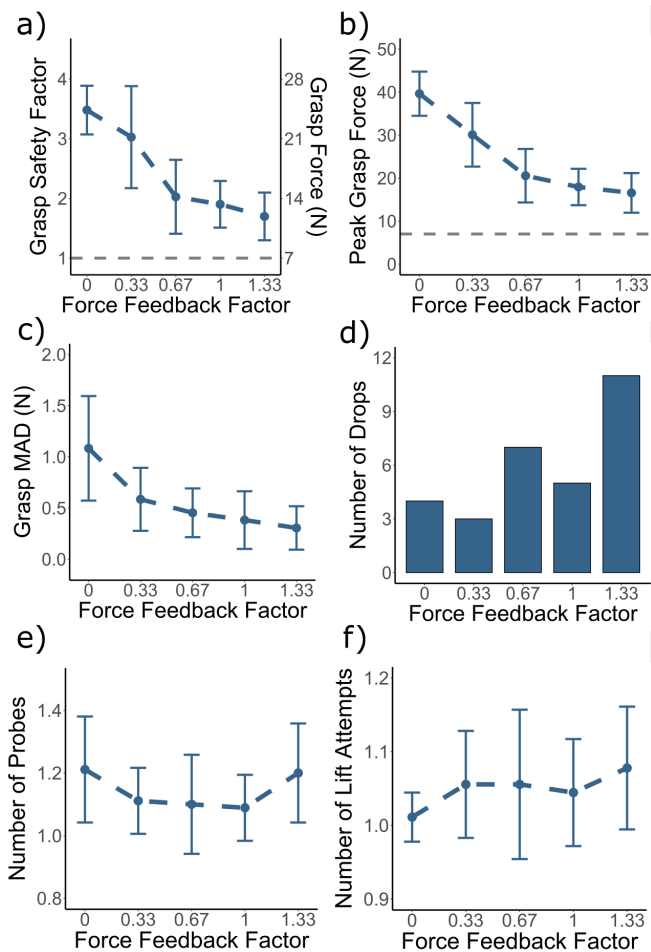


Fig. 6. Summary of data on grasp performance metrics: a) Overall mean grasp force in newtons and safety factor across all participants at each force factor. b) Overall mean peak grasp force in Newtons across all participants at each force factor. c) Overall mean Mean Absolute Deviation (MAD) of grasp hold force across all participants at each force factor. d) Number of drops out of 90 total trials between all participants at each force factor. e) Overall mean number of probes prior to the hold region across all participants at each force factor. f) Overall mean number of lift attempts prior to the hold region across all participants at each force factor. Error bars denote standard deviation of subject means at each force factor.

IV. RESULTS

A. Grasp Economy

Participants are better able to regulate their grasp force while holding the virtual test object as the force feedback factor increased, shown in Fig. 6(a). Their grasp safety factor, defined as the ratio between the mean grasp force and minimum force required for lift-off, reduces by more than a factor of two between the lowest and highest displayed force feedback factors. Analysis of the LMM shows a significant effect of force feedback factor on mean grasp force ($b = -0.318$, $p = 0.004$) but no significant effect of factor order ($b = 0.043$, $p = 0.167$).

Analysis also reveals a significant two-way interaction between force feedback factor and factor order ($b = -0.101$,

¹The 95% factor accounts for potential slight inaccuracies in hold region estimation and helps limit false positives.

$p = 0.002$), indicating an increased ability to control grasp force using force feedback as more factors are experienced. Change in mean grasp force across trials in a single factor is small, with no significant two-way or three-way interactions ($FO \cdot T$: $b = 0.001$, $p = 0.645$; $K_f \cdot FO \cdot T$: $b = 0.002$, $p = 0.503$), suggesting a minimal within-factor learning effect.

B. Peak Grasp Force

The data similarly show a decrease in peak grasp force as force feedback factor increases, seen in Fig. 6(b), dropping from 39.6 N at no feedback to 16.6 N at maximum feedback. This is supported by a significant effect of force feedback factor ($b = -0.597$, $p < 0.001$). The covariate of factor order does not appear to have a significant effect on peak force ($b = 0.032$, $p = 0.345$) but does have a significant interaction with force feedback factor ($K_f \cdot FO$: $b = -0.101$, $p = 0.010$), again indicating an increasing sensitivity to force feedback as more factors are experienced. The LMM analysis also shows slight within-factor effects with significant two- and three-way trial interactions ($FO \cdot T$: $b = -0.006$, $p = 0.013$; $K_f \cdot FO \cdot T$: $b = 0.009$, $p = 0.005$), though their magnitudes are small and conflict in direction.

C. Grasp Steadiness

Participants maintain a steadier grasp force while holding the test object as force feedback factor increases. This effect is shown in the decrease in grasp mean absolute deviation (MAD), in Fig. 6(c), from 1.08 N at no feedback to 0.31 N at maximum feedback through the hold phase. From the findings of the LMM, this outcome appears to be driven predominantly by the significant effect of force feedback factor ($b = -0.756$, $p < 0.001$) and changes only slightly with the covariate of factor order ($b = 0.047$, $p = 0.610$) or their interaction ($K_f \cdot FO$: $b = -0.106$, $p = 0.340$). Trial has no significant effect on grasp MAD in two- or three-way interactions ($FO \cdot T$: $b = 0.002$, $p = 0.831$; $K_f \cdot FO \cdot T$: $b = 0.000$, $p = 0.981$).

D. Drop Rate

Participants drop the test object while in the hold region more often at higher force feedback factors, shown in Fig. 6(d). A drop rate of 4.44% (4 drops out of 90 trials) occurs with no force feedback ($K_f = 0$), while a drop rate of 12.2% (11 drops out of 90 trials) occurs at the highest tested force feedback factor ($K_f = 1.33$). Results from the binomial regression model indicate a significant effect of force feedback factor ($b = 0.887$, $p = 0.036$). No other significant effects are found, whether directly from other covariates (FO : $b = 0.184$, $p = 0.607$) or from any two- or three-way interactions ($K_f \cdot FO$: $b = -0.301$, $p = 0.442$; $FO \cdot T$: $b = -0.069$, $p = 0.139$; $K_f \cdot FO \cdot T$: $b = 0.058$, $p = 0.256$).

E. Probes and Lift Attempts

Participants perform a mean number of probes between 1 and 1.21 and a mean number of lift attempts between 1 and

1.1 for all cases, seen in Fig. 6(e,f). GLM analysis for probe number indicates no significant effect of force feedback factor ($b = -0.174$, $p = 0.416$), factor order ($b = -0.006$, $p = 0.933$), or their interaction ($K_f \cdot FO$: $b = 0.093$, $p = 0.278$). It also shows no significant interaction effects for trial ($FO \cdot T$: $b = -0.008$, $p = 0.333$; $K_f \cdot FO \cdot T$: $b = -0.007$, $p = 0.510$). Analysis for number of lift attempts shows a similar lack of significant effects for predictors, covariates, and interactions (K_f : $b = 0.041$, $p = 0.856$; FO : $b = 0.006$, $p = 0.944$; $K_f \cdot FO$: $b = 0.005$, $p = 0.959$; $FO \cdot T$: $b = 0.000$, $p = 0.961$; $K_f \cdot FO \cdot T$: $b = -0.001$, $p = 0.912$). Thus, it appears that changes in force feedback factor do not cause participants to vary their interaction with the virtual object prior to the hold region.

V. DISCUSSION

Individuals apply lower grasping forces, closer to the required minimum for lifting the object, and maintain steadier grasps while holding the test object with higher levels of force feedback. This outcome aligns with work done with individuals performing normative grasping experiments with anesthetized hands, leading subjects to apply over twice as much pinch force during lifting trials than under non-anesthetized conditions. [23], [25]. At the same time, our results extend the findings beyond related works on kinesthetic feedback in upper-limb body-powered prostheses [20], [21], [29] by describing the effect on grasping across a continuous spectrum of kinesthetic feedback conditions.

A non-linear relationship appears to exist between our chosen performance metrics (grasp safety factor, peak force, MAD) and the force feedback factor. For all three metrics, the differences between higher levels of force feedback are smaller than those at lower levels of feedback. This suggests the potential for a significant improvement in grasp force moderation using only light or moderate forces displayed, with diminishing returns at high forces. This motivates the use of smaller and lighter motors for the active display of feedback forces, since outputting high feedback forces might only result in modest grasp performance gains. This would be of particular importance for the integration of force feedback into the design of many haptic and wearable technologies where minimizing the weight and size of haptic actuators is essential for usability.

Participants exert the lowest mean grasp force when the force feedback factor is highest, thus achieving the smallest safety margin out of all experimental conditions. Additionally, more intense feedback exerts more load on the shoulder during operation, potentially leading to larger than intended or unexpected motions of the shoulder if the muscles relax. This, combined with the smaller margin for error, could influence the higher drop rate observed at high feedback forces. Further experimentation with a narrower focus on producing drop events during prosthesis operation would be necessary to draw more specific causal conclusions and is left for future work. Regardless, the existence of the trend itself provides reason for caution from arbitrarily raising the magnitudes of displayed forces.

Direct generalizability of the findings to physical grasping is somewhat limited by the non-physical nature of the interactions via a virtual environment. We limited the information regarding applied grasp forces to only the forces displayed through the shoulder harness and visual perception of the simulated grasping environment in order to focus the experiment on the primary independent variable of interest, the feedback factor. Notably, the height controller did not allow for the perception of weight or vibratory sensations of slip that might allow users to better scale their grasp forces, as has been shown to be the case for normative grasping [23], [30], [31]. Future work will explore how the effects we observe thus far are influenced by physical interaction during grasping. This could also lead to additional insights into motor learning and dynamic force control in the context of real-world wearable technologies with kinesthetic feedback. The integrated nature of control and feedback modalities in body-powered prostheses also complicates the generalization of these results to other devices with separate control schemes like myoelectric prostheses. Additional work could evaluate the function of kinesthesia as solely a feedback modality alongside a different control input like EMG activity.

VI. CONCLUSION

Through systematically varying the level of force feedback presented to users through a body-powered prosthesis emulator, we evaluated its role in the regulation and control of grasp force. The additional sensory knowledge of a grasp state provided through force feedback allows individuals to better apply predictable and stable internal grasp forces while interacting with their environment. Yet, the increased loads applied to their bodies also render them more prone to drops as well as the fatigue and discomfort typical of body-powered prosthesis use over longer periods of time. This suggests that moderate levels of grasp force feedback via cable-driven systems may be able to maximize grasp performance for extensive usage.

Further investigation could also lead towards the design of novel assistive technologies. Hybrid upper-limb prostheses, for example, could take advantage of the enhanced control of the EPP topology while limiting physical loads on the body using active elements. The application of EPP to new contexts, such as for users with intact but deficient limbs as with stroke, also holds potential to see innovative devices which operate in parallel with peripheral motor systems. It is our intention that this work may help to inform the integration of kinesthetic feedback into future research and designs for assistive and prosthetic devices.

ACKNOWLEDGMENT

Michael Abbott was supported by the National Science Foundation Graduate Research Fellowship Program (award number DGE 1752814). The authors acknowledge the support of Richard Nguyen, the UCSF Department of Orthopaedic Surgery, and the members of the Embodied Dexterity Group.

REFERENCES

- [1] D. Datta, K. Selvarajah, and N. Davey, "Functional outcome of patients with proximal upper limb deficiency-acquired and congenital," *Clinical Rehabilitation*, vol. 18, no. 2, pp. 172-177, Mar. 2004, publisher: SAGE Publications Ltd STM. [Online]. Available: <https://doi.org/10.1191/0269215504cr7160a>
- [2] F. Cordella, A. L. Ciancio, R. Sacchetti, A. Davalli, A. G. Cutti, E. Guglielmelli, and L. Zollo, "Literature Review on Needs of Upper Limb Prosthesis Users," *Frontiers in Neuroscience*, vol. 10, May 2016. [Online]. Available: <https://www.ncbi.nlm.nih.gov/pmc/articles/PMC4864250/>
- [3] "bebionic hand." [Online]. Available: <https://www.ottobockus.com/prosthetics/upper-limb-prosthetics/solution-overview/bebionic-hand/>
- [4] "i-Limb@ Ultra." [Online]. Available: <https://www.ossur.com/en-us/prosthetics/arms/i-limb-ultra/prosthetics/arms/i-limb-ultra>
- [5] "Hero Arm - an affordable, advanced and intuitive bionic arm." [Online]. Available: <https://openbionics.com/hero-arm/>
- [6] E. A. Biddiss and T. T. Chau, "Upper limb prosthesis use and abandonment: A survey of the last 25 years," *Prosthetics and Orthotics International*, vol. 31, no. 3, pp. 236-257, Jan. 2007. [Online]. Available: <https://www.tandfonline.com/doi/abs/10.1080/03093640600994581>
- [7] E. Biddiss, D. Beaton, and T. Chau, "Consumer design priorities for upper limb prosthetics," *Disability and Rehabilitation: Assistive Technology*, vol. 2, no. 6, pp. 346-357, Jan. 2007. [Online]. Available: <https://doi.org/10.1080/17483100701714733>
- [8] H. J. Witteveen, H. S. Rietman, and P. H. Veltink, "Vibrotactile grasping force and hand aperture feedback for myoelectric forearm prosthesis users," *Prosthetics and Orthotics International*, vol. 39, no. 3, pp. 204-212, Jun. 2015, publisher: SAGE Publications Ltd STM. [Online]. Available: <https://doi.org/10.1177/0309364614522260>
- [9] A. E. Pena, L. Rincon-Gonzalez, J. J. Abbas, and R. Jung, "Effects of vibrotactile feedback and grasp interface compliance on perception and control of a sensorized myoelectric hand," *PLOS ONE*, vol. 14, no. 1, p. e0210956, Jan. 2019, publisher: Public Library of Science. [Online]. Available: <https://journals.plos.org/plosone/article?id=10.1371/journal.pone.0210956>
- [10] M. A. Schweisfurth, M. Markovic, S. Dosen, F. Teich, B. Graimann, and D. Farina, "Electrotactile EMG feedback improves the control of prosthesis grasping force," *Journal of Neural Engineering*, vol. 13, no. 5, p. 056010, Aug. 2016, publisher: IOP Publishing. [Online]. Available: <https://doi.org/10.1088%2F1741-2560%2F13%2F5%2F056010>
- [11] S. Dosen, M. Markovic, M. Strbac, M. Belić, V. Kojić, G. Bijelić, T. Keller, and D. Farina, "Multichannel Electrotactile Feedback With Spatial and Mixed Coding for Closed-Loop Control of Grasping Force in Hand Prostheses," *IEEE Transactions on Neural Systems and Rehabilitation Engineering*, vol. 25, no. 3, pp. 183-195, Mar. 2017, conference Name: IEEE Transactions on Neural Systems and Rehabilitation Engineering.
- [12] S. Casini, M. Morvidoni, M. Bianchi, M. Catalano, G. Grioli, and A. Bicchi, "Design and realization of the CUFF - clenching upper-limb force feedback wearable device for distributed mechano-tactile stimulation of normal and tangential skin forces," in *2015 IEEE/RSJ International Conference on Intelligent Robots and Systems (IROS)*, Sep. 2015, pp. 1186-1193.
- [13] K. R. Schoepp, M. R. Dawson, J. S. Schofield, J. P. Carey, and J. S. Hebert, "Design and Integration of an Inexpensive Wearable Mechanotactile Feedback System for Myoelectric Prostheses," *IEEE Journal of Translational Engineering in Health and Medicine*, vol. 6, pp. 1-11, 2018, conference Name: IEEE Journal of Translational Engineering in Health and Medicine.
- [14] K. J. Zuo and J. L. Olson, "The evolution of functional hand replacement: From iron prostheses to hand transplantation," *Plastic Surgery*, vol. 22, no. 1, pp. 44-51, 2014. [Online]. Available: <https://www.ncbi.nlm.nih.gov/pmc/articles/PMC4128433/>
- [15] S. L. Carey, D. J. Lura, M. J. Highsmith, CP, and FAAOP, "Differences in myoelectric and body-powered upper-limb prostheses: Systematic literature review," *Journal of Rehabilitation Research and Development*, vol. 52, no. 3, pp. 247-262, 2015. [Online]. Available: <http://www.rehab.research.va.gov/jour/2015/523/pdf/JRRD-2014-08-0192.pdf>
- [16] P. S. Lum, I. Black, R. J. Holley, J. Barth, and A. W. Dromerick, "Internal models of upper limb prosthesis users when grasping and lifting a fragile object with their prosthetic limb," *Experimental Brain Research*, vol. 232, no. 12, pp. 3785-3795, Dec. 2014. [Online]. Available: <https://doi.org/10.1007/s00221-014-4071-1>
- [17] J. M. Romano, S. R. Gray, N. T. Jacobs, and K. J. Kuchenbecker, "Toward tactilely transparent gloves: Collocated slip sensing and vibrotactile actuation," in *World Haptics 2009 - Third Joint Euro-Haptics conference and Symposium on Haptic Interfaces for Virtual Environment and Teleoperator Systems*, Mar. 2009, pp. 279-284.
- [18] D. Simpson and others, "The choice of control system for the multimovement prosthesis: extended physiological proprioception (epp)," *The control of upper-extremity prostheses and orthoses*, pp. 146-150, 1974, publisher: Charles C. Thomas.
- [19] J. A. Doubler and D. S. Childress, "An analysis of extended physiological proprioception as a prosthesis-control technique," *Journal of rehabilitation research and development*, vol. 21, no. 1, pp. 5-18, 1984.
- [20] J. D. Brown, T. S. Kunz, D. Gardner, M. K. Shelley, A. J. Davis, and R. B. Gillespie, "An Empirical Evaluation of Force Feedback in Body-Powered Prostheses," *IEEE Transactions on Neural Systems and Rehabilitation Engineering*, vol. 25, no. 3, pp. 215-226, Mar. 2017.
- [21] A. Filatov and O. Celik, "Effects of body-powered prosthesis prehensory stiffness on performance in an object stiffness discrimination task," in *2015 IEEE World Haptics Conference (WHC)*, Jun. 2015, pp. 339-344.
- [22] M. Hichert, A. N. Vardy, and D. Plettenburg, "Fatigue-free operation of most body-powered prostheses not feasible for majority of users with trans-radial deficiency," *Prosthetics and Orthotics International*, vol. 42, no. 1, pp. 84-92, Feb. 2018. [Online]. Available: <https://www.ncbi.nlm.nih.gov/pmc/articles/PMC5808823/>
- [23] R. Johansson and G. Westling, "Roles of glabrous skin receptors and sensorimotor memory in automatic control of precision grip when lifting rougher or more slippery objects," *Experimental Brain Research*, vol. 56, no. 3, Oct. 1984. [Online]. Available: <http://link.springer.com/10.1007/BF00237997>
- [24] D. A. Nowak, J. Hermsdörfer, S. Glasauer, J. Philipp, L. Meyer, and N. Mai, "The effects of digital anaesthesia on predictive grip force adjustments during vertical movements of a grasped object," *European Journal of Neuroscience*, vol. 14, no. 4, pp. 756-762, 2001. [Online]. Available: <https://onlinelibrary.wiley.com/doi/abs/10.1046/j.0953-816x.2001.01697.x>
- [25] J. Monzée, Y. Lamarre, and A. M. Smith, "The Effects of Digital Anesthesia on Force Control Using a Precision Grip," *Journal of Neurophysiology*, vol. 89, no. 2, pp. 672-683, Feb. 2003. [Online]. Available: <https://www.physiology.org/doi/full/10.1152/jn.00434.2001>
- [26] R Core Team, *R: A Language and Environment for Statistical Computing*. Vienna, Austria: R Foundation for Statistical Computing, 2019. [Online]. Available: <https://www.R-project.org/>
- [27] J. Pinheiro, D. Bates, S. DebRoy, D. Sarkar, and R Core Team, *nlme: Linear and Nonlinear Mixed Effects Models*, 2020. [Online]. Available: <https://CRAN.R-project.org/package=nlme>
- [28] D. Bates, M. Mächler, B. Bolker, and S. Walker, "Fitting Linear Mixed-Effects Models Using lme4," *Journal of Statistical Software*, vol. 67, no. 1, pp. 1-48, 2015.
- [29] J. D. Brown, A. Paek, M. Syed, M. K. O'Malley, P. A. Shewokis, J. L. Contreras-Vidal, A. J. Davis, and R. B. Gillespie, "Understanding the role of haptic feedback in a teleoperated/prosthetic grasp and lift task," in *2013 World Haptics Conference (WHC)*, Apr. 2013, pp. 271-276.
- [30] R. S. Johansson and G. Westling, "Coordinated isometric muscle commands adequately and erroneously programmed for the weight during lifting task with precision grip," *Experimental Brain Research*, vol. 71, no. 1, pp. 59-71, Jun. 1988. [Online]. Available: <https://doi.org/10.1007/BF00247522>
- [31] J. Hermsdörfer, Y. Li, J. Randerath, G. Goldenberg, and S. Eidenmüller, "Anticipatory scaling of grip forces when lifting objects of everyday life," *Experimental Brain Research*, vol. 212, no. 1, pp. 19-31, Jul. 2011. [Online]. Available: <https://doi.org/10.1007/s00221-011-2695-y>